AN EXTENDED SET-VALUED OBSERVER FOR POSITION ESTIMATION USING SINGLE RANGE MEASUREMENTS

José Marçal, Jérôme Jouffroy and Thor I. Fossen
Department of Engineering Cybernetics
Norwegian University of Science and Technology
NO-7491 Trondheim, Norway
E-mail: marcal@itk.ntnu.no, jerome.jouffroy@ntnu.no, fossen@ieee.org

***Abstract*— The ability of estimating the position of an underwater vehicle from single range measurements is important in applications where one transducer marks an important geographical point, when there is a limitation in the size or cost of the vehicle, or when there is a failure in a system of transponders.**

The knowledge of the bearing of the vehicle and the range measurements from a single location can provide a solution which is sensitive to the trajectory that the vehicle is following, since there is no complete constraint on the position estimate with a single beacon. In this paper the observability of the system is briefly discussed and an extended set-valued observer is presented, with some discussion about the effect of the measurements noise on the final solution. This observer estimates bounds in the errors assuming that the exogenous signals are bounded, providing a safe region of confidence where the underwater vehicle is located.

I. Introduction

Navigation plays a very important role in autonomous underwater vehicles (AUVs) and it is a critical factor when considering a task to be performed. The setup time for a mission, the cost and the required accuracy are the factors that engineers have to weight in order to choose the best configuration of sensors for the navigation solution. Typically the vehicle contains sensors which allow to compute an accurate solution for a short period of time (dead-reckoning), such as inertial navigation systems (INS), propeller speed measurement and compass. The aid of a Doppler velocity log (DVL) to an INS system is a current solution in high accuracy systems, leading to larger periods where only the onboard sensors are used to compute the position, velocity and attitude (PVA). Typically, position errors of a few meters per hour can be achieved by these systems [13], [12], [4].

In order to bound these growing errors, measurements relative to a known location are used. If the task of the AUV is to be performed at low depths, the signals provided by a GPS receiver can be used. In underwater environments, the good propagation of acoustic waves makes the acoustic transducers the usual choice for reference stations that provide absolute navigation points, although magnetic and optical technology is also used for shorter distances, for example in homing or docking maneuvers [7], [1], [9]. Despite the good propagation properties in water of the acoustic waves, their vulnerability to undesired effects such as multipath create a challenge in signal processing techniques, and the spurious measurements have to be rejected using outlier rejection techniques [20]. The normal assumptions of pure Gaussian noise may be unsuitable for a system which relies only on the Kalman filter framework.

The interest in navigation systems that rely just on one transponder as a position reference does not appear only as a safety need, but also makes underwater exploration more versatile. The development of USBL systems was due to the demands of the offshore industry, in order to provide another navigation reference, but it is also used in AUVs, as shown in [16]. The difference in phase of the different measurements is used to compute the line of sight vector from the AUV to the transponder and the time of flight of the acoustic pulse gives information about the range . Homing and docking with a single range information have also been object of study, as in the works of Vaganay [11]. In this case, a circular maneuver is done by the AUV to observe the position vector, which, although efficient, is not needed, as Gadre and Stilwell [10] have shown on their theoretical study on observability in navigation systems based on range measurements from a single location. They proofed that the system is observable if both the speed and the angular velocity of the AUV are non-zero. MARIDAN introduced the synthetic baseline concept [14]. With the knowledge of the bearing information they were able to correct the drifting errors of the high accuracy INS/DVL system MARPOS [13]. Although this was an efficient approach to navigation with one transducer, low cost navigation sensors on board the AUV may require a much more careful analysis of the observability of the system to prevent the vehicle of going to some unwanted locations. The 3σ-ellipsoidal confidence region given by the extended Kalman filter (EKF), although used in many systems when considering the worst case scenario, may not be accurate enough due to the non-linearities of the model and the partial observability in this problem.

A set-valued observer estimates the possible states based on output measurements and models of exogenous signals which are bounded. Due to the increasing computing power and the sub-performance of the Kalman filter in non-linear systems or in systems where the noise is not Gaussian, there has been a lot of interest lately in this approach to estimation problems. The paper from Bertsekas [2] is the basic reference in set-membership description of uncertainty; Shamma and Tu [18], [19] showed that set-valued estimation provides optimal estimates in the $\mathcal{H}_\infty$-induced norm sense and Calafiore [5]

presented some algorithms to implement the observer, mainly based on the work of Boyd et al. [3], which introduced the linear matrix inequalities (LMI) framework to this problem. In this work, this latter implementation is considered, with some analogies to the Kalman filter approach, using LMIs. The problem is formulated as two semidefinite programs that are to be solved. Recent progresses in the LMI theory made this approach more attractive with the computational complexity of the same order as the EKF [6], [3]. This observer provides bounds to the estimated position error that take into account the worst case scenarios, when the statistical description of the measurement noise is not correct, which may happen when the acoustic signals arrive to the receiver in multiple paths, for example. This is a more robust estimation method than the traditional Kalman filtering. However, the estimated trajectories are not as smooth as in the latter, in general.

In this paper, the focus goes to an absolute positioning system consisting of one transponder, which provides information to the vehicle, bounding the errors present in the dead reckoning navigation. This is implemented using a set-valued observer. In Section II, a brief observability study gives the geometric interpretation of the problem and provides some considerations about the problem of navigating with just one transponder. Section III presents the theoretical background on the observer. Some comparisons between the classical EKF approach and this observer are done in Section IV, based on some simulations, and a conclusion is given in Section V.

II. Observability Analysis

Without loss of generality, the 3D navigation solution of an AUV can be studied just in the x-y plane, while a depth sensor provides the z-axis information. Typically, the z-axis position estimation is done by combining that measurement and the acceleration and/or velocity in that direction. By measuring the time-of-flight of the acoustic signal, and knowing *a priori* the location of the transponder, the range projection on the x-y plane can be expressed by:

$$\rho = \sqrt{\rho_m^2 - (\Delta z_m)^2} \tag{1}$$

where Δz_m is the difference between the transponder and the vehicle depths and ρ_m is the measured range between the vehicle and the transponder. Assuming that the roll and pitch angles do not influence the horizontal motion, the system in the x-y plane can be written in terms of the state variables $[\ x(t) \quad y(t) \quad \psi(t)\ ]$ and the measurement equation $h_{xy}(t)$, where $\psi(t)$ is the vehicle heading and $r(t)$ is the yaw rate, as follows:

$$\Sigma_1 : \begin{bmatrix} \dot{x}(t) \\ \dot{y}(t) \\ \dot{\psi}(t) \end{bmatrix} = \begin{bmatrix} v(t).\cos(\psi(t)) \\ v(t).\sin(\psi(t)) \\ r(t) \end{bmatrix} \tag{2}$$

$$h_{xy}(t) = \begin{bmatrix} \sqrt{x(t)^2 + y(t)^2} \\ \psi(t) \end{bmatrix} \tag{3}$$

For the analysis present in this paper, no considerations about biases or scale factors are done, although those should be estimated and used to correct the sensors used for dead-reckoning. In order to study the observability of the system, and to give a better geometrical insight of the problem, it is convenient to represent the state variables in terms of polar coordinates

$$\Sigma_2 : \begin{bmatrix} \dot{\rho}(t) \\ \dot{\theta}(t) \\ \dot{\psi}(t) \end{bmatrix} = \begin{bmatrix} v(t).\cos(\psi(t) - \theta(t)) \\ \frac{v(t)}{\rho(t)}.\sin(\psi(t) - \theta(t)) \\ r(t) \end{bmatrix} \tag{4}$$

$$h(t) = \begin{bmatrix} h_1(t) \\ h_2(t) \end{bmatrix} = \begin{bmatrix} \rho(t) \\ \psi(t) \end{bmatrix} \tag{5}$$

A system is said to be observable if for any two states $q_1(t)$, $q_2(t)$ there exists an admissible control $u \in \mathcal{U}$ and a time $t \geq 0$ such that $y_{q_1,u(t)}(t) \neq y_{q_2,u(t)}(t)$, which means that these states are distinguishable [17] . The measurement equations of the system Σ_2 are the distance to the transponder and the yaw angle, which are, therefore, two observable states of the system. To study the observability of $\theta(t)$, it is necessary to study the derivatives of the measurement equation along the solutions of Σ_2, which are the Lie derivatives of the function $h(t)$ with respect to the the vector field on the right side of equation (4). From the Lie derivatives of h_2, no information about θ can be achieved directly. However, combining those with the derivatives of h_1, a solution can be computed. If there is a change in the yaw angle, the second derivative of h_1, provided that there is a knowledge about the values of ρ and ψ (which is verified as those are the direct measurements) can be used to compute θ, under the condition that $r \neq 0$ and $v \neq 0$.

$$\begin{aligned} L_f^{(1)} h_1 &= v.\cos(\psi - \theta) \\ L_f^{(2)} h_1 &= v.\sin(\psi - \theta).r - \frac{v^2}{\rho}.\sin^2(\psi - \theta) \end{aligned} \tag{6}$$

Clearly, from the equations, if $r = 0$ there exist two functions $\theta_1(t)$ and $\theta_2(t)$, symmetric along the line where $\psi = \theta$ that produce the same output $h(t)$ independently of the number of derivatives of $h(t)$ that are considered (see Figure 1). In this case the system is not distinguishable. This case can be avoided by forcing the vehicle to do some maneuvers, which will result in no ambiguity when deciding which of the trajectories is the true one. If the vehicle is subjected to large accelerations, the system should be augmented, in which case an external accelerometer would be used to directly observe the velocity rate, or, in case of a smooth trajectory, the assumption of constant velocity may be a good approximation. In this work the latter is assumed.

There is always an admissible control vector where $r(t)$ is not identically zero that discerns which one of the solutions is true. However, as these two trajectories become closer, the measurements noise (specially in the yaw angle) may lead to wrong corrections. This is due to the fact that these two trajectories minimize the square error of the difference

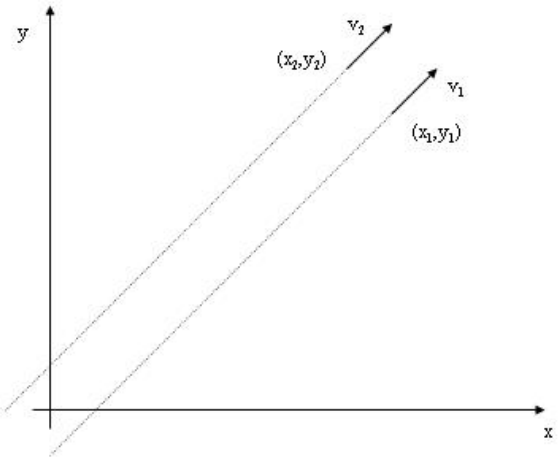

Fig. 1. Two indistinguishable trajectories. The yaw angle and the distance to the transponder are equal in both cases at each time sample.

between the real and the predicted measurements, as illustrated in Figure 2. Even with very low rate turns this situation may happen, as long as a sequence of bad measurements is received and the difference between ψ and θ is small. In this case the two solutions that satisfy the observability equation are too close and such makes them hardly distinguishable. When using a Kalman filter, the confidence ellipsoid may not include the true solution, leading to a wrong but coherent estimation, in the sense that the wrong trajectory also minimizes $(y - Cx)^T(y - Cx)$. By using more a relaxed confidence region, assuming that a bounded value of noise may affect the system, this situation can be avoided.

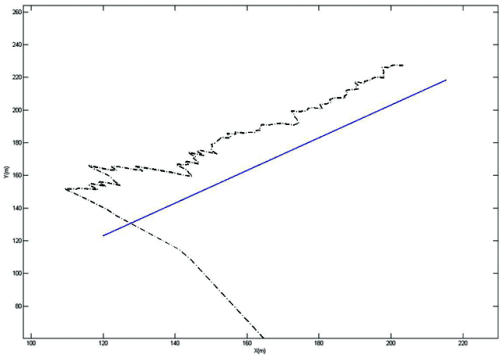

Fig. 2. Estimate (dotted) and true (solid) trajectories. Due to the noise and to the proximity of the points that satisfy the measurement equation the estimate may not be correct.

The problems discussed above lead to the need of a more robust estimation method, which is guaranteed to contain the true state of the system. Although the new observer may subperform when compared to the Kalman filter in some cases, its robustness to the non-linearities of the system and to the measurement noise, which may not be Gaussian, present some attractive points in severe environments.

III. Set-Valued observer design

In order to design the observer, the algorithm presented in [5] is considered. Using the equation (2), it is assumed that the sampled dynamics are described by:

$$x_{k+1} = f(x_k, u_k) + B_k w_k \tag{7}$$

where w_k is a noise vector which is unknown-but-bounded (UBB), $\|w_k\| < 1$, and B_k is a scaling matrix. Similarly, the measurement equation is

$$y_k = h(x_k, u_k) + D_k v_k \tag{8}$$

where v_k and D_k have analogous meaning as w_k and B_k.

A set-valued observer estimates the states from the assumption that the disturbances are bounded. In this case, similarly to the Kalman filter approach, there is a prediction and a correction step in the observer. In the prediction step, a bounding ellipsoid, centered in $x_{k+1|k}$ and with limits given by $E_{k+1|k}$ is to be computed, which is guaranteed to contain the state of the system at the next step, if proper values of noise and linearization errors are chosen. The following equation is used:

$$x_{k+1} = (A_k + L_a\Delta_a)(x_k - \hat{x}_k) + B_k w_k + f(\hat{x}_k, u_k) \tag{9}$$

This equation is linearized about the central estimate $\hat{x}_k$, and model uncertainties and non-linearities are expressed by the matrices L_a and Δ_a. A_k is defined as $\partial f(x,u)/\partial x$ at the point $\hat{x}_k$, while L_a is a scaling matrix and Δ_a a matrix which takes into account the errors in the model due to non-linearities or inaccuracies in the model, such that $\|\Delta_a\| \leqslant 1$. These last two matrices are obtained assuming that the uncertainties in the model admit a linear fractional representation [8]. In order to convert this problem into a LMI problem, and using the results of [5], the following semidefinite program (SDP) is to be solved, in terms of the variables $P_{k+1|k}, \tau_z, \tau_w, \tau_a$:

$$\text{minimize } Tr(P_{k+1|k}) \tag{10}$$

subject to

$$\begin{gathered} \begin{bmatrix} P_{k+1|k} & \Phi(\hat{x}_{k+1|k}) \\ \Phi^T(\hat{x}_{k+1|k}) & \Omega(\tau_z, \tau_w, \tau_a) \end{bmatrix} > 0 \\ \tau_z, \tau_w, \tau_a > 0 \\ P_{k+1|k} > 0 \end{gathered} \tag{11}$$

where

$$\Phi = \begin{bmatrix} f(\hat{x}_k, u_k) - \hat{x}_{k+1|k} & A_k E_k & B_k & L_a \end{bmatrix} \tag{12}$$

$$\Omega = diag(1 - \tau_z - \tau_w, \tau_z I - \tau_a E_k^T E_k, \tag{13}$$

$$\tau_w I, \tau_a I) \tag{14}$$

These results were derived from the $\mathcal{S}$-procedure (see [5] for details). The matrix $P_{k+1|k}$ is the positive definite matrix that defines the uncertainty ellipsoid after the measurements, while τ_z,τ_w and τ_a are positive integers resulting from the $\mathcal{S}$-procedure, introducing some extra robustness [3]. When solving this SDP, basically there is an approximation of the summing of all the uncertainty ellipsoids to a single ellipsoid that is certain to include all the possible bounded disturbances. This way a simple semidefinite problem can be stated and solved using efficient numerical methods, instead of working with a complex polytope. The prediction step is, in this case, very similar to the one in the EKF, only that it is expressed as an LMI.

The correction step is written in an analogous way, with the output equation of the system being

$$\begin{aligned} y_{k+1} &= (C_{k+1} + L_c\Delta_c)(x_{k+1} - \hat{x}_{k+1|k}) + \\ &\quad D_k v_k + h(\hat{x}_{k+1|k}) \end{aligned} \tag{15}$$

where the matrices L_c and Δ_c are the scaling factor and a matrix that takes into account the non-linear terms of the measurement equation respectively. At this step we are given the ellipsoid that is certain to contain the true state

$$x_{k+1} = f(x_k, u_k) + B_k z_k \tag{16}$$

for some z_k such that $\|z_k\| < 1$. To obtain the set of states that satisfy both the measurement equation and the ellipsoidal bounds, a SDP is defined as follows:

$$\text{minimize } Tr(P_{k+1}) \tag{17}$$

subject to

$$\begin{gathered} \left[\begin{array}{cc} P_{k+1|k} & \Phi_m(\hat{x}_{k+1})\Psi \\ \Psi^T\Phi_m^T(\hat{x}_{k+1}) & \Psi^T\Omega_m(\tau_z,\tau_v,\tau_c)\Psi \end{array} \right] > 0 \\ \tau_z, \tau_v, \tau_c > 0 \\ P_{k+1} > 0 \end{gathered} \tag{18}$$

where

$$\Phi_m = [\ \hat{x}_{k+1|k} - \hat{x}_{k+1} \quad E_{k+1|k} \quad 0 \quad 0\ ] \tag{19}$$

$$\begin{aligned} \Omega_m = diag(&1 - \tau_z - \tau_v, \tau_z I - \tau_c E_{k+1|k}^T E_{k+1|k}, \\ &\tau_v I, \tau_c I) \end{aligned} \tag{20}$$

This comes from the fact that the measurement equation can be expressed as

$$[\ h(\hat{x}_{k+1|k}) - y_{k+1} \quad C_{k+1}E_{k+1|k} \quad D \quad L_c\ ] \left[\begin{array}{c} 1 \\ z^T \\ v^T \\ p_c^T \end{array} \right] = 0 \tag{21}$$

which can be written as

$$\Phi_y[\ 1 \quad z^T \quad v^T \quad p_c^T\ ]^T = 0 \tag{22}$$

All the vectors satisfying 22 can be expressed as the product of the orthogonal complement of Φ_y, which is Ψ, with another vector. As in the KF framework, this orthogonal complement limits the search of the solutions to the straight line between the measured value and the estimated measurement and provides a way to fuse information with different statistics. With the SDP (18), an ellipsoid is to be found which bounds the intersection of the predicted ellipsoid and the set of values which are compatible with the measurement equation, which are defined by multiplying Φ_m with Ψ.

The type of noise in LBL systems is mainly Gaussian (see [21]), with some outages which can be considered as exogenous signals to the system. Therefore, the bounds of the signals can be compared to their "Gaussian equivalent" in terms of variance. For the case of an uniform distribution over an interval of length Δ, the computed variance is equal to $\Delta^2/12$. If the noise distribution is Gaussian, then a scaling factor of $\sqrt{12}$ is to be used in the matrices, which means that in this observer the scaling matrices can be taken as the covariance matrices of the Kalman filter multiplied by $\sqrt{12}$. In that case, with those bounds on the exogenous signals, a confidence interval of about 99% is guaranteed. However, if strong non-linearities are present, or if the model of the system has some uncertainties, this interval of confidence is no longer valid. A wrong calibration of the process noise may lead to the divergence of the filter, due to a false assumption of the certainty interval. By assuming larger bounds and taking all the possible solutions based on the measurements, a robust estimator is designed which is not as smooth as the Kalman filter but is not so sensitive to measurements with low accuracy.

IV. Simulation results

In all the simulations, it is assumed that the acoustic signal of the transponder is received every $10s$. The range measurements are affected by a Gaussian noise with a variance equal to $1m^2$ and the compass variance is about $(0, 6^\circ)^2$. The velocity of the vehicle is measured with an accuracy of $0, 1m/s$ RMS, sampled each second. The matrices B and D of the LMI observer are obtained from the measurement noise and the process noise covariance matrices from the Kalman filter, multiplying them by a factor of $\sqrt{12}$.

1) Straight line: In this case, the AUV is moving without changing its direction. The problem of this maneuver is mainly the weak observability at long distances from the transponder. Figures 3, 4 and 5 show the results of the simulation. Although in terms of central estimate the two solutions present similar results, it is interesting that, when looking at the 3σ-ellipsoid of the EKF and the confidence ellipsoid of the LMI observer, as the distance to the transponder becomes larger, there are some periods of time where the first one does not include the true value of the position, while the second one always includes the real position (see Fig.4).

It can be seen that the estimates of the extended Kalman filter are smoother than the ones from the LMI observer

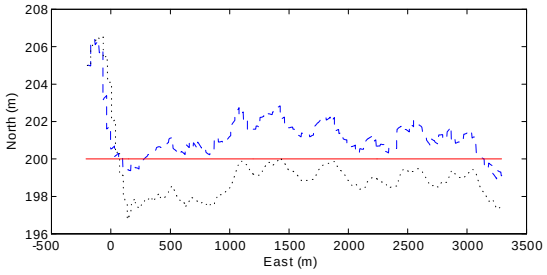

Fig. 3. Simulated straight line trajectory. The solid line is the real trajectory and the dashed and dotted lines are the EKF and the LMI observer estimations.

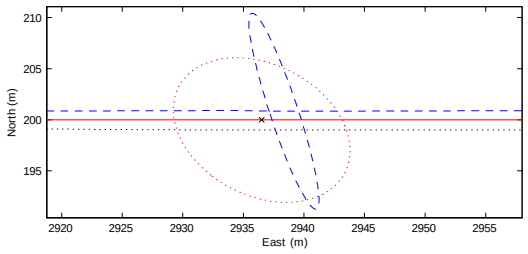

Fig. 4. Confidence region for both filters. The cross is the real position, while the dashed and dotted ellipsoids are the EKF and the LMI observer regions of confidence.

(Fig.5), and that is particularly noticeable for the yaw angle. In fact, this is expected, since the solution of the EKF should be, approximately, since the system is non-linear, the one that minimizes the variance of the error. However, the flexibility of the LMI observer, where the smoothness part is sacrificed in order to have a high confidence on the bounding ellipsoid, may be an important factor when the interest is on the certainty of the position.

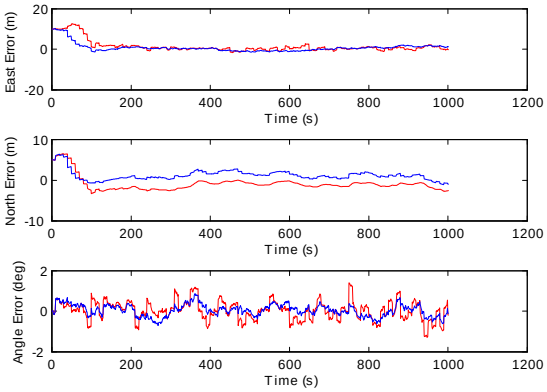

Fig. 5. Estimation errors of the EKF (dark line) and the LMI estimator (light line) for the straight line case.

2) Lawn-mower trajectory: The lawn-mowing trajectory is typical when using sensors for which this geometry cancels some bias which is present, for example, in DVL systems. Although with a good inertial system following a straight line can be very accurate [13], the turns can still be a problem, due to the discretization and the centripetal forces that actuate on the AUV. In this simulation, the Kalman filter solution is, once more, the smoother one; however, that is more noticeable in the north position, where the LMI observer is more sensitive to the measurement noise (see Fig.8). Observing the east position error, both filters have similar results. In terms of the region of confidence, the 3σ-ellipsoids of the EKF, although generally accurate in this maneuver, are not correct at some points (see Fig.7).

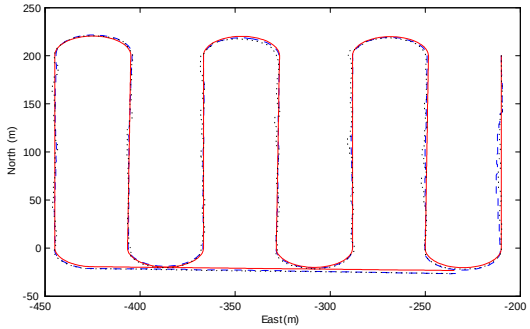

Fig. 6. Simulated lawn-mowing trajectory. The solid line is the real trajectory and the dashed and dotted lines are the EKF and the LMI observer estimations.

In mapping applications this smoothness is necessary in order to acquire good images, making the EKF the usual choice. However, the implementation of the LMI observer may be used to consider possible errors in the final solution, in post-mission processing, instead of the usual resort to the bounds provided by the EKF.

3) Lawn-mower with some non-Gaussian measurements: When the measurement noise is Gaussian, it is naturally expected that the EKF would obtain the best results, which is generally true in terms of point estimation (this is, the center

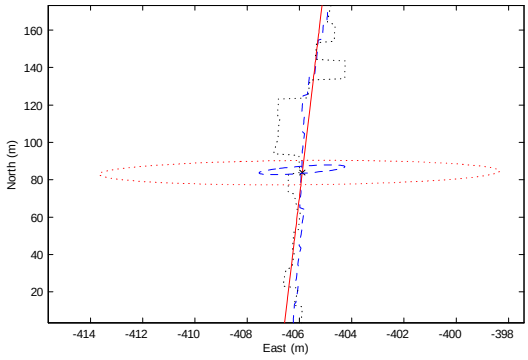

Fig. 7. Zoom to a portion of the lawn-mowing maneuver. The true value is signaled with a cross, the confidence ellispoids of the EKF and the LMI observer are dashed and dotted respectively.

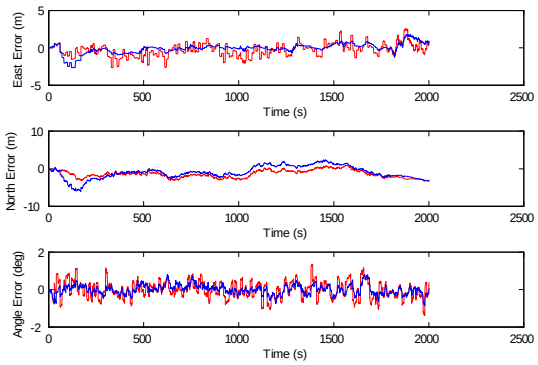

Fig. 8. Estimation errors of the EKF (dark line) and the LMI estimator (light line) in the lawn-mowing maneuver.

of the ellipsoids is closer to the true value), although some bad sets of data may degrade its performance. In some missions, however, the noise in the range measurements may not be well modelled as a Gaussian noise. Due to multipath effects, for example, the noise probability distribution may not be so simple to describe. Based on some LBL noise figures [21], this simulation presents the lawn-mower trajectory where, during a period of time in the trajectory, the measurement noise is the sum of a Gaussian noise with an uniform distribution in the interval $[-\sigma, \sigma]$. Usually, outlier detection techniques are designed to avoid these perturbations [20], but it is not straightforward to decide whether a measurement is valid or not when, for example, multiple path signals have a similar energy to the signal and are not far apart in time [15].

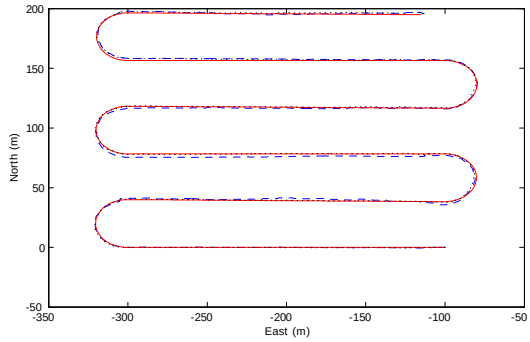

Fig. 9. Simulated lawn-mowing trajectory with some bad measurements. The solid line is the real trajectory and the dashed and dotted lines are the EKF and the LMI observer estimations.

In the simulation this non-Gaussian noise was added in the period of time between $500s$ and $600s$, exactly before a turning maneuver, where the measurements are of absolute importance because of the change in the yaw angle. As seen in Figure 10 in the north position error, the EKF is more affected by this disturbances, having almost a constant bias, which is corrected only on the next turn. Graphically, Figure 11 illustrates the two estimates and the real trajectory when this perturbations

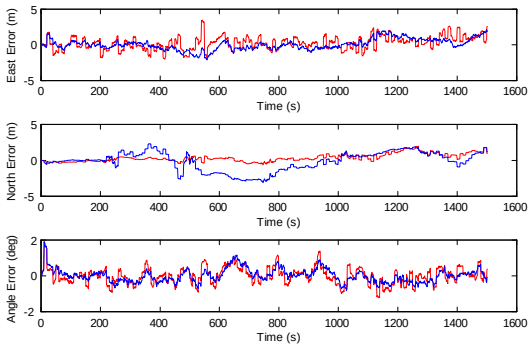

Fig. 10. Estimation errors of the EKF (dark line) and the LMI estimator (light line) in the lawn-mowing maneuver with non-Gaussian noise during a period of time.

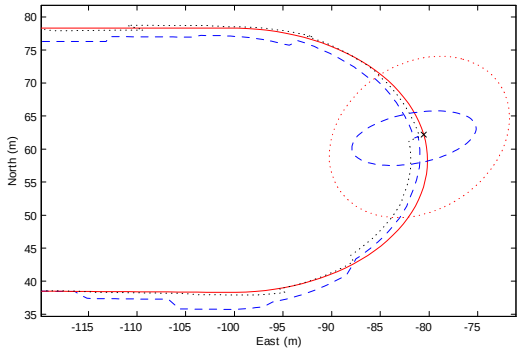

Fig. 11. Zoom to a portion of the lawn-mowing maneuver where some bad measurements affected the estimation; the true value is signaled with a cross, the confidence ellispoids of the EKF and the LMI observer are dashed and dotted respectively.

occur, together with the bounding ellipsoids at one specific sample. Although both of them are correct in terms of regions of confidence, the LMI point estimate has almost zero mean error, while the Kalman solution is smoother but also affected by a temporary bias.

V. Conclusion

In this paper, a set-valued observer for navigation with single range measurements is presented. This observer accounts for the non-linearities of the model and presents a good performance when the statistics of the signal are not accurately known, even if just on a small part of the trajectories, where the acoustic signal may be subjected to multiple paths. This approach may be important when an absolute certainty of the error bounds is required, which is an important factor in critical tasks. It may be also a tool for post-processing, estimating bounds more accurately than the EKF.

VI. Acknowledgment

The authors would like to acknowledge the people at the Centre of Ships and Ocean Structures (CESOS) and the

Department of Engineering Cybernetics at NTNU for the constructive comments and suggestions. The Norwegian Research Council is also acknowledged as the main sponsor.

REFERENCES

[1] A. Balasuriya and T. Ura. Sensor fusion technique for cable following by autonomous underwater vehicles. In *Proc. OCEANS'1999*, pages 1779–1785, Hawaii, USA, Aug. 1999.

[2] D. P. Bertsekas and I. B. Rhodes. Recursive state estimation for a set-membership description of uncertainty. *IEEE Transactions on Automatic Control*, 16:117–128, Feb. 1971.

[3] S. Boyd, L. El Ghaoui, E. Feron, and V. Balakrishnan. Linear matrix inequalities in system and control theory. In *Proc. Annual Allerton Conf. on Communication, Control and Computing*, Allerton House, Monticello, Illinois, Oct. 1993.

[4] B. Butler and R. Verral. Precision hybrid inertial/acoustic navigation system for a long-range autonomous underwater vehicle. *Journal of the Institute of Navigation*, 48(1):1–12, 2001.

[5] G. Calafiore. Reliable localization using set-valued nonlinear filters. *IEEE Transactions on systems, man and cybernetics*, 35:189–197, Mar. 2005.

[6] G. Calafiore and L. E. Ghaoui. Ellipsoidal bounds for uncertain linear equations and dynamical systems. *Automatica*, 50:773–787, 2004.

[7] S. Cowen, S. Briest, and J. Dombrowski. Underwater docking of autonomous undersea vehicles using optical terminal guidance. In *Proc. OCEANS'1997*, pages 1143–1147, Kauai, Hawaii, USA, Oct. 1997.

[8] L. El Ghaoui and G. Calafiore. Robust filtering for discrete-time systems with bounded noise and parametric uncertainty. *IEEE Transactions on Automatic Control*, 46(7):1084–1089, 2001.

[9] M. Feezor, F. Y. Sorrel, P. Blankinship, and J. Bellingham. Autonomous underwater vehicle homing/docking via electromagnetic guidance,. *IEEE Journal of Oceanic Engineering*, 26(4):515–521, 2001.

[10] A. S. Gadre and D. Stilwell. Toward underwater navigation based on range measurements from a single location. In *Proc. IEEE International Conference on Robotics and Automation*, pages 4472–4477, New Orleans, LA, Apr. 2004.

[11] B. J. J. Vaganay, P. Baccou. Homing and navigation using one transponder for auv, post-processing comparisons results with long baseline navigation. In *IEEE International Conference on Robotics and Automation*, pages 4004–4009, 2002.

[12] B. Jalving, K. Gade, K. Svartveit, A. Willumsen, and R. Sørhagen. DVL velocity aiding in the HUGIN 1000 integrated inertial navigation system. *Modeling, Identification and Control*, 25(4):223–235, 2004.

[13] M. Larsen. High performance doppler-inertial navigation - experimental results. In *Proc. OCEANS'2000*, pages 1449–1456, Rhode Island Convention Center, Sept. 2000.

[14] M. Larsen. Synthetic long baseline navigation of underwater vehicles. In *Proc. OCEANS'2000*, pages 2043–2050, Rhode Island Convention Center, Sept. 2000.

[15] X. Lurton. *An Introduction to Underwater Acoustics*. Springer-Praxis, Chichester, UK, 2002.

[16] F. Parthiot and J. Denis. A better way to navigate on deep sea floors. In *Proc. OCEANS'1993*, pages 494–498, New York, 1993.

[17] W. Respondek. Geometry of static and dynamic feedback, 2001. Lecture notes.

[18] J. Shamma and K.-Y. Tu. Approximate set-valued observers for nonlinear systems. *IEEE Transactions on Automatic Control*, pages 648–658, May 1997.

[19] J. Shamma and K.-Y. Tu. Set-valued observers and optimal disturbance rejection. *IEEE Transactions on Automatic Control*, pages 253–264, Feb. 1999.

[20] S. Vike and J. Jouffroy. Diffusion-based outlier rejection for underwater navigation. In *IEEE Marine Technology and Ocean Science Conference (OCEANS'2005)*, 2005. To appear.

[21] L. L. Whitcomb, D. R. Yoerger, H. Singh, and D. A. Mindell. Towards precision robotic maneuvering, survey, and manipulation in unstructured undersea environments. In Y. Shirai and S. Hirose, editors, *Robotics Research - The Eighth International Symposium*, pages 45–54. Springer-Verlag, London, 1998.